Electronic Supporting Information (ESI)

Proton conductivity dependence on surface polymer thickness of weak acidic polymer-coated core-shell type nanoparticles for proton exchange membrane

Keisuke Tabata,[a] Tomohiro Nohara,[a] Haruki Nakazaki,[a] Tsutomu Makino,[a] Takaaki Saito,[a] Toshihiko Arita[b] and Akito Masuhara*[a, c]*

[a] Graduate School of Science and Engineering, Yamagata University, 4-3-16 Yonezawa, Yamagata 992-8510, Japan.

[b] Institute of Multidisciplinary Research for Advanced Materials (IMRAM), Tohoku University, 2-1-1 Katahira, Aoba-ku, Sendai, Miyagi 980-8577, Japan.

[c] Frontier Center for Organic Materials (FROM), Yamagata University, 4-3-16 Jonan, Yonezawa, Yamagata 992-8510, Japan.

Toshihiko Arita*

E-mail: tarita@tohoku.ac.jp

Akito Masuhara*

E-mail: masuhara@yz.yamagata-u.ac.jp

Synthesis of xanthate type RAFT agent (X_1)

The chain transfer agent (CTA) used for RAFT/MADIX polymerization of PVPA was prepared by a simple reaction. *o*-ethyl-*S*-(1-ethoxycarbonyl)-ethyldithiocarbonate (X_1) which is CTA was obtained by mixing equimolar ethyl-2-bromopropionate (EBP) and potassium ethylxanthate (PEX), stirring overnight at 0 ° C in ethanol (Scheme S1).[1, 2] After the reaction, the desired product was extracted using a mixed solvent of diethyl ether and pentane (2: 1) and water, then, water was removed with magnesium sulfate. After that, magnesium sulfate used for dehydration was removed by filtration. The liquid state product was purified by an evaporator to obtain X_1 in a yellow liquid state. The structure of the obtained X_1 was confirmed by ^{1}H NMR and stored in a refrigerator (Fig. S1).

Scheme S1 Synthesis scheme of X_1.

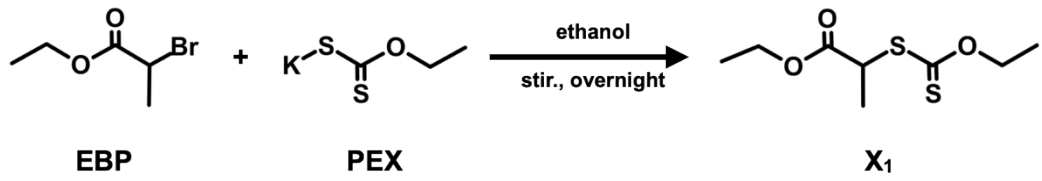

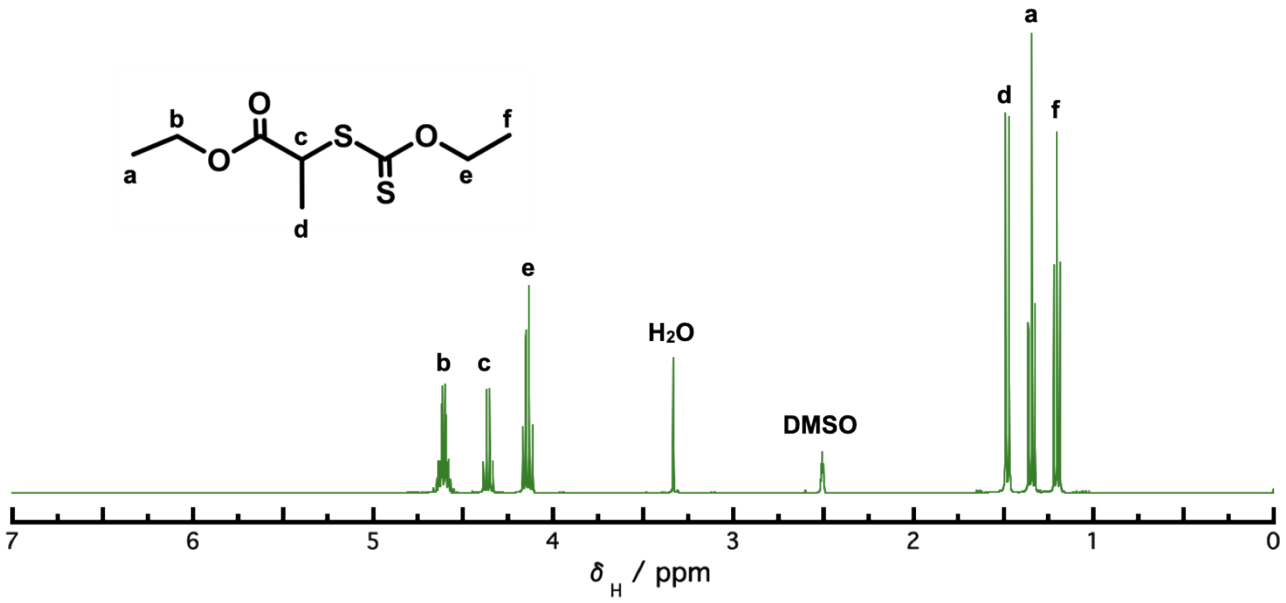

Fig. S1 ^{1}H NMR spectrum of X_1.

RAFT/MADIX polymerization of PVPA

The polymerization of PVPA was evaluated using ^{1}H and ^{31}P nuclear magnetic resonance (NMR; JEOL), and DMSO-*d*6 was used as a deuterated solvent at the time of measurement. The RAFT/MADIX polymerization of PVPA was carried out at a constant monomer-to-CTA-to-initiator feed ratio ($[VPA]_0/[CTA]_0/[AIBN]_0$ = 100:1:0.4) in DMF at 65℃ and various polymerization time (3, 6, 12, 18, 24, 48 h). The ^{1}H NMR and ^{31}P NMR spectra of each sample were measured using DMSO-*d*6 as the heavy solvent (Fig. S2).

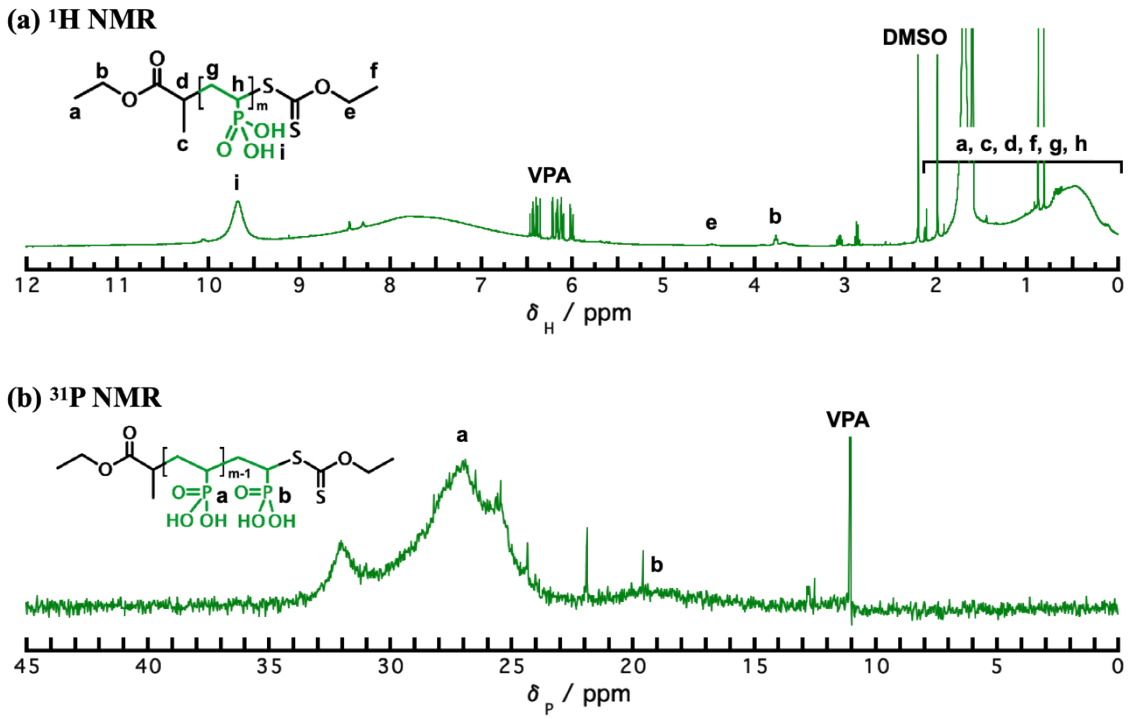

Fig. S2 (a) ^{1}H and (b) ^{31}P NMR analysis of PVPA.

From ^{1}H NMR spectra, a broad peak appeared at 0.5-2.0 ppm, confirming that PVPA polymerization proceeded. In addition, since the signals derived from the terminal methylene of X1 used as CTA were observed at 4.6 and 4.1 ppm, it can be said that the RAFT/MADIX polymerization of PVPA was proceeded by X1. ^{31}P NMR was used to calculate the VPA conversion for RAFT/MADIX polymerization. Signals for VPA monomer, VPA unit adjacent to X1, and PVPA were observed at 11.2, 20, and near 30 ppm, respectively. From the above, the VPA conversion can be easily determined by using the integral ratios of these signals using this formula:

$$VPA\ conversion\ [\%] = \frac{(VPA\ unit\ adjacent\ to\ X_1\ +\ polymer)}{(VPA +\ VVPA\ unit\ adjacent\ to\ X_1\ +\ polymer)}$$

As a result of RAFT / MADIX polymerization of PVPA performed in DMF solvent, the VPA conversion rate was 50% at 24 hours and 58% at 48 hours, which is lower than the VPA polymerization conversion rate shown in previous studies (Fig. S3).[3, 4] In fact, a lower VPA conversion rate of RAFT/MADIX polymerization compared with the ancient free radical polymerization has been a problem also in previous studies. *L. Seiler et al.* clarified the tendency of electrostatic repulsion of VPA (monomer) and PVPA (polymer) to delay polymerization and reported a study to improve the polymerization conversion rate by adding counter ions. However, our study needed to consider not only electrostatic repulsion but also the influence of DMF solvent on the delay of polymerization. According to Z. Taherkhani *et al.*[5] hydrophilic VPA is polymerized by solution polymerization in water and polymerized by precipitation polymerization in solvents such as DMF and ethyl acetate. Therefore, polymerization in water gives a higher molecular weight. In contrast, we sued DMF as a polymerization solvent to promote the RAFT PwP which requires a combination of core nanoparticles and solvent to be phase-separated. Resulting in the VPA conversion decreased compared to using water.

In this research, we examined only polymerization time fixed with the ratio of [VPA]0 / [CTA]0 = 100/1. However, to reduce the loss by further improving the VPA conversion, further studies such as monomer-to-CTA-to-initiator feed ratio and polymerization temperature are necessary.

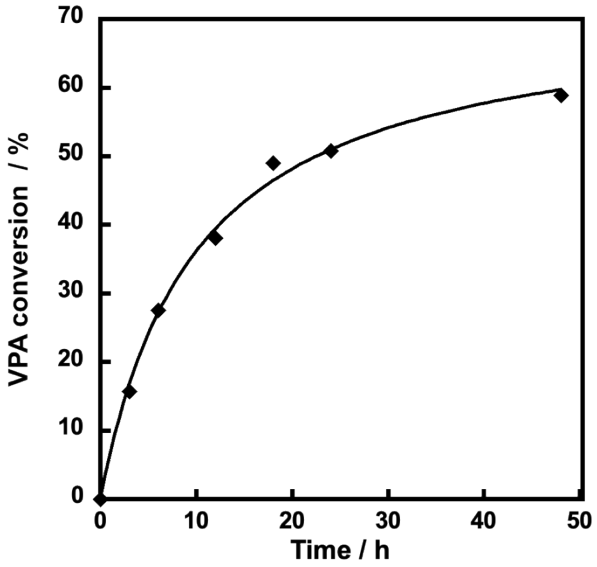

Fig. S3 Time-conversion curves during the RAFT/MADIX polymerization of VPA using X_1.

SEM images

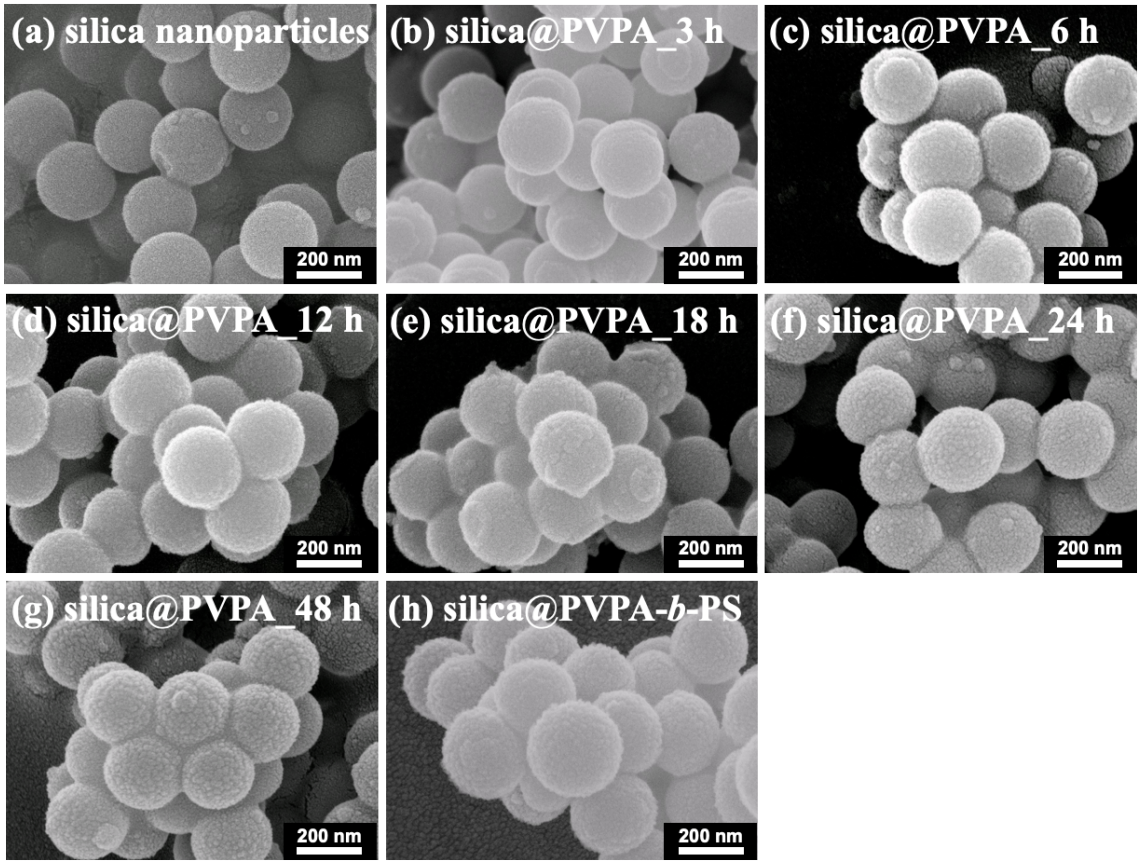

Fig. S4 FE-SEM images of (a) bare silica nanoparticles with a diameter of 200 nm, (b)–(g) silica@PVPA with various PVPA polymerization times (3 h–48 h), and (h) silica@PVPA-*b*-PS.

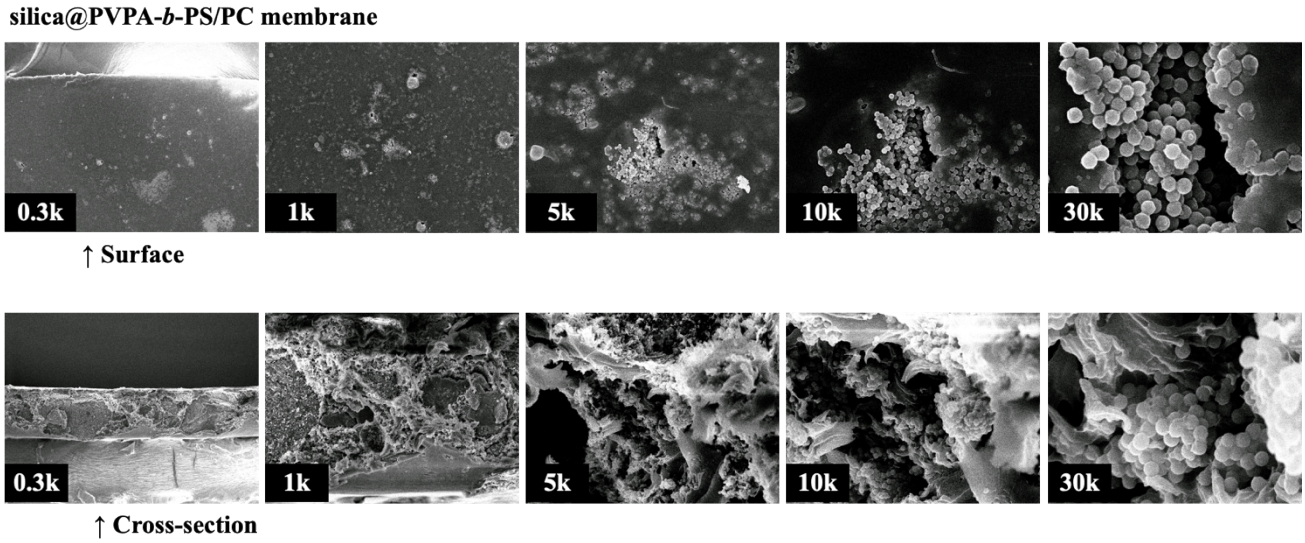

Fig. S5 silica@PVPA-*b*-PS/PC membrane surface and cross-section.

FTIR spectra

In order to clarify the coating of PVPA and PS on the surface of silica nanoparticles, we measured FTIR and described FTIR spectra in Fig. S6 and Fig. S7. FTIR measurement was performed by the KBr tablet method.

We intentionally saturated the absorption originating from the silica nanoparticles at 1300-1800 cm-1 and observed the absorption derived from PVPA. PVPA shows broad P=O absorption at 1300–1150 cm^{-1} and P-OH at 1010–800 cm^{-1}, however, these absorptions overlap with the absorptions of silica nanoparticles. These absorptions were not adequate to discriminate the PVPA coating. Silica@PVPA showed noticeable absorptions compared with bare silica nanoparticles such as P=OH stretching vibration at 1624 cm^{-1} and absorption of C-H scissors vibration of the main chain methylene group at 1470 cm^{-1}. In silica@PVPA-*b*-PS, some absorptions derived from the aromatic ring were observed. Aromatic C-H expansion and contraction vibrations were observed at 3030 cm^{-1}, C-C expansion and contraction vibrations of the aromatic ring were observed at 1490 and 1450 cm^{-1}, and sharp peaks due to C-H out-of-plane bending vibrations were observed at 700 cm^{-1}.[6-8]

In addition, we normalized the absorption attributed to core silica nanoparticles at 800cm^{-1}, then, observed the vibration of O=P-OH groups of silica@PVPA (polymerization time: 3-48 h) at 1650 cm^{-1} (Fig. S8). The absorption intensity derived from PVPA was gradually increased as the polymerization time became longer. Therefore, the thickness of PVPA onto the surface of silica nanoparticles was increased.

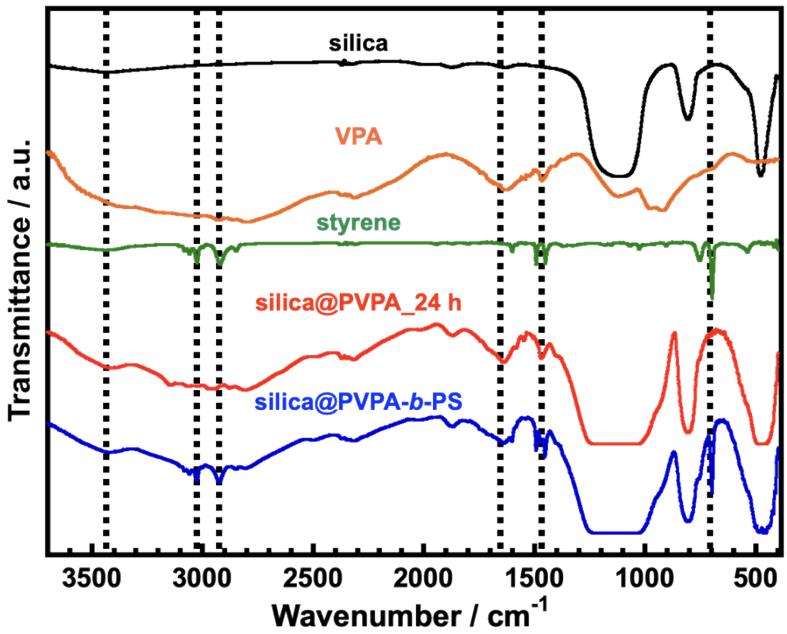

Fig. S6 FTIR spectra of bare silica nanoparticles, VPA, styrene, silica@PVPA_24 h, and silica@PVPA-*b*-PS.

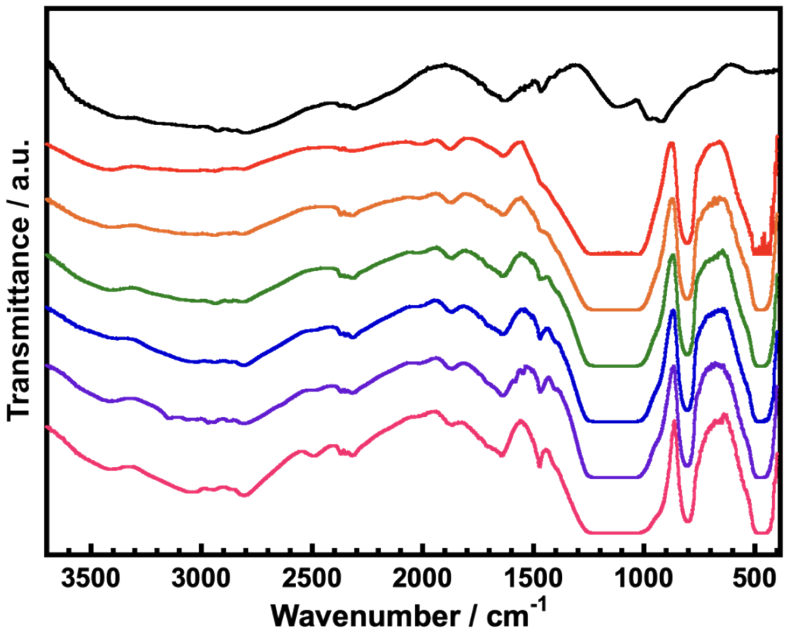

Fig. S7 FTIR spectra of silica@PVPA (3, 6, 12, 18, 24, 48 h).

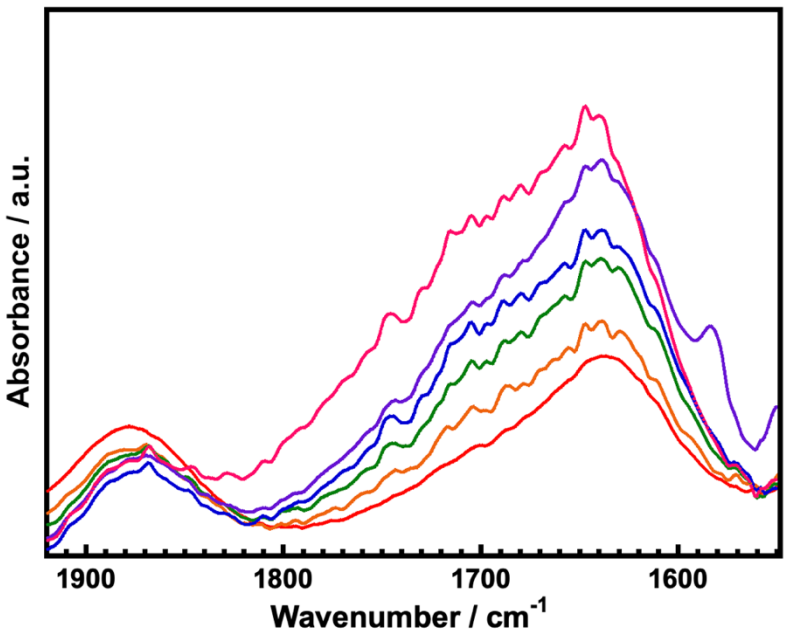

Fig. S8 FTIR spectra of silica@PVPA (3, 6, 12, 18, 24, 48 h).

TGA curves

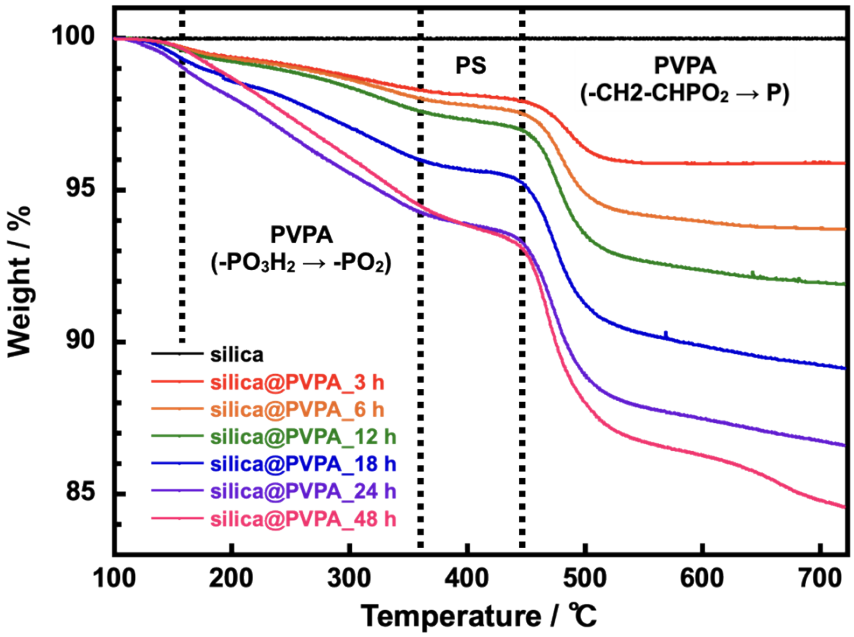

Fig. S9 TGA curves of silica and silica@PVPA (3, 6, 12, 18, 24, 48 h).

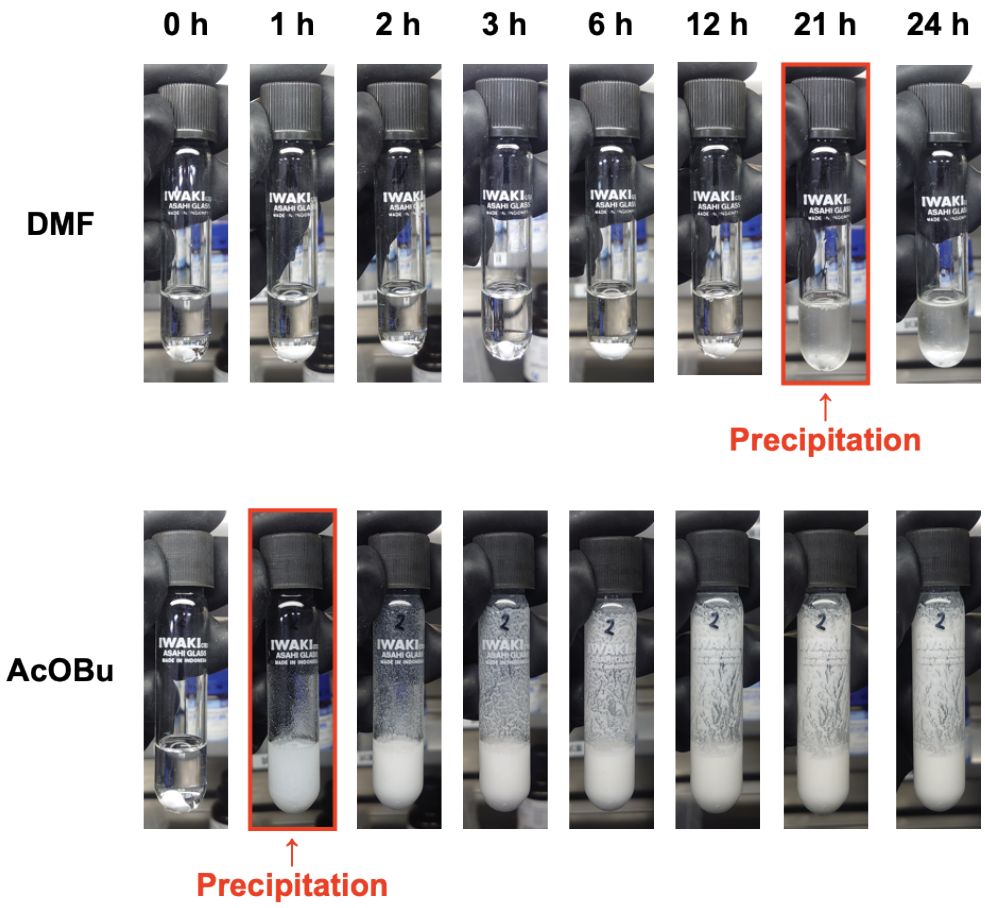

Fig. S10 Photos of PVPA polymerization using DMF and AcOBu as solvent.

UV-vis spectra

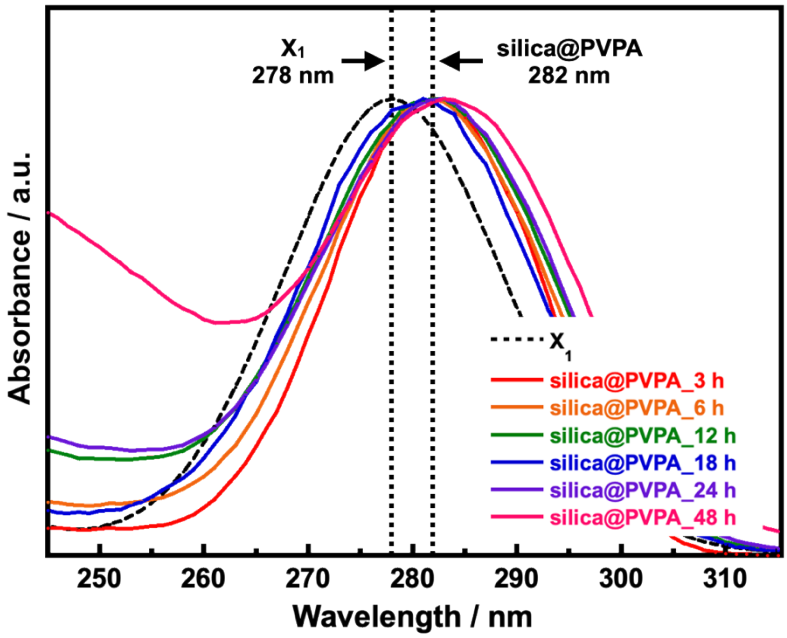

Fig. S11 The Kubelka-Munk transformation of the reflectance curves of silica@PVPA (3, 6, 12, 18, 24, and 48 h).

Cole-Cole plot

(a) silica@PVPA_3 h

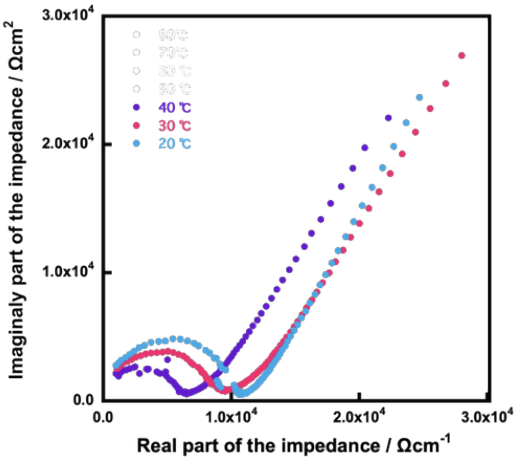

(b) silica@PVPA_6 h

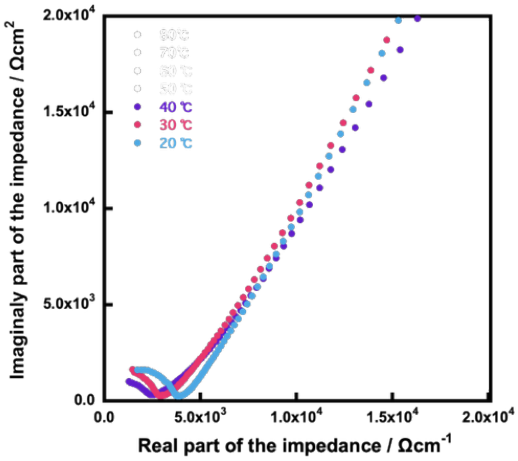

(c) silica@PVPA_12 h

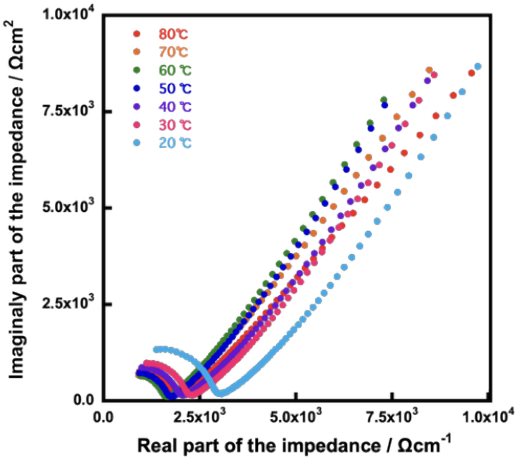

(d) silica@PVPA_18 h

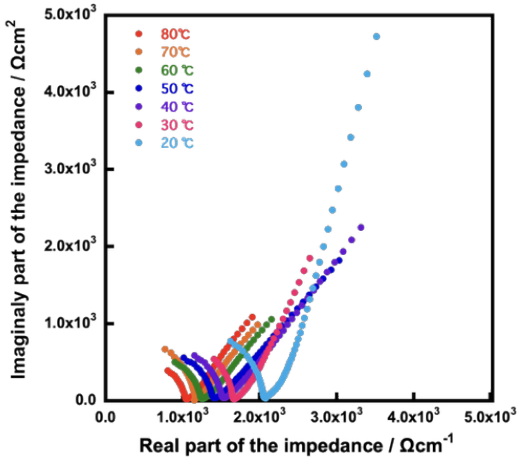

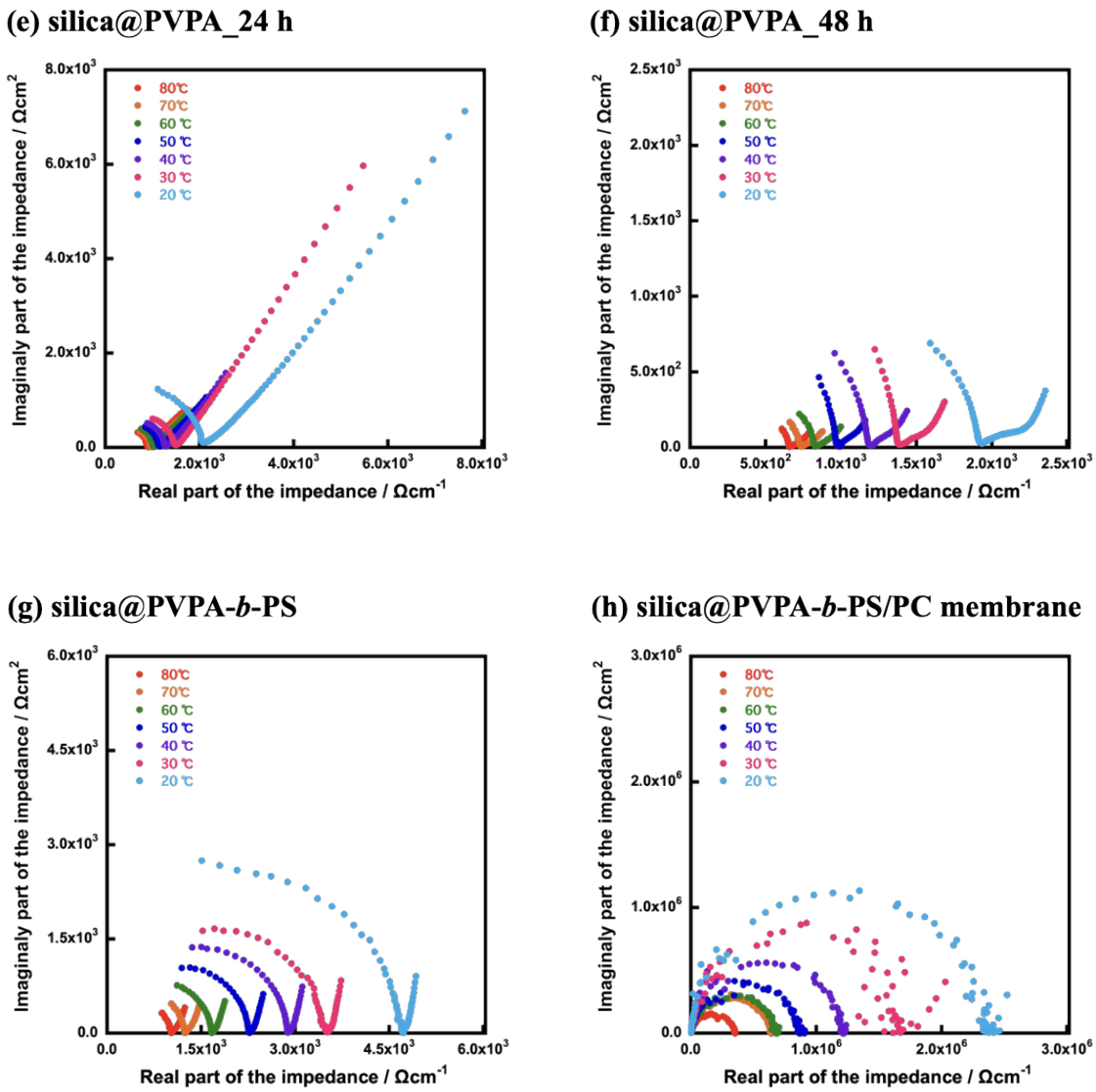

Fig. S12 Cole-Cole plots of (a) silica@PVPA_3 h, (b) silica@PVPA_6 h, (c) silica@PVPA_12 h, (d) silica@PVPA_18 h, (e) silica@PVPA_24 h, (f) silica@PVPA_48 h, (g) silica@PVPA-*b*-PS, and (h) silica@PVPA-*b*-PS/PC membrane.

Table S1 Temperature dependence of proton conductivities of each sample measured at 20℃–80℃ and 95% RH.

sample	Temperature / ℃, 95% RH							E_a / eV (95% RH)
	20	30	40	50	60	70	80	
silica@PVPA_3 h	8.9×10^{-4}	1.0×10^{-3}	1.5×10^{-3}	-	-	-	-	0.23
silica@PVPA_6 h	2.7×10^{-3}	3.6×10^{-3}	4.2×10^{-3}	-	-	-	-	0.21
silica@PVPA_12 h	5.7×10^{-3}	7.6×10^{-3}	8.6×10^{-3}	1.0×10^{-2}	1.1×10^{-2}	1.0×10^{-2}	9.1×10^{-3}	0.10
silica@PVPA_18 h	8.1×10^{-3}	1.0×10^{-2}	1.1×10^{-2}	1.2×10^{-2}	1.3×10^{-2}	1.5×10^{-2}	1.6×10^{-2}	0.12
silica@PVPA_24 h	8.5×10^{-3}	1.2×10^{-2}	1.4×10^{-2}	1.6×10^{-2}	1.7×10^{-2}	1.8×10^{-2}	2.0×10^{-2}	0.14
silica@PVPA_48 h	1.5×10^{-2}	2.1×10^{-2}	2.4×10^{-2}	3.0×10^{-2}	3.5×10^{-2}	4.0×10^{-2}	4.4×10^{-2}	0.18
silica@PVPA-*b*-PS	2.9×10^{-3}	3.9×10^{-3}	4.7×10^{-3}	6.0×10^{-3}	8.2×10^{-3}	1.1×10^{-2}	1.3×10^{-2}	0.26
silica@PVPA-*b*-PS/PC membrane	6.8×10^{-5}	8.9×10^{-5}	1.0×10^{-4}	1.2×10^{-4}	1.4×10^{-4}	1.7×10^{-4}	1.8×10^{-4}	0.18

Table S2 Humidity dependence of proton conductivities each sample measured at 80℃ and 30% RH–95% RH.

sample	80℃, RH / %							
	30	40	50	60	70	80	90	95
silica@PVPA_24 h	1.0×10^{-5}	3.7×10^{-5}	1.1×10^{-4}	3.3×10^{-4}	9.1×10^{-4}	2.7×10^{-3}	9.5×10^{-3}	2.2×10^{-2}
silica@PVPA-*b*-PS	5.8×10^{-6}	2.4×10^{-5}	8.1×10^{-5}	2.3×10^{-4}	7.2×10^{-4}	2.2×10^{-3}	7.4×10^{-3}	1.5×10^{-2}
silica@PVPA-*b*-PS/PC membrane	-	-	-	3.4×10^{-6}	1.2×10^{-5}	4.8×10^{-5}	1.4×10^{-4}	2.7×10^{-4}

References

1. S. Perrier and P. Takolpuckdee, *Journal of Polymer Science Part A: Polymer Chemistry*, 2005, **43**, 5347-5393.
2. R. M. Moraes, L. T. Carvalho, G. M. Alves, S. F. Medeiros, E. Bourgeat-Lami and A. M. Santos, *Polymers (Basel)*, 2020, **12**, 1252.
3. I. Blidi, R. Geagea, O. Coutelier, S. Mazières, F. Violleau and M. Destarac, *Polymer Chemistry*, 2012, **3**, 609-612.
4. L. Seiler, J. Loiseau, F. Leising, P. Boustingorry, S. Harrisson and M. Destarac, *Polymer Chemistry*, 2017, **8**, 3825-3832.
5. Z. Taherkhani, M. Abdollahi and A. Sharif, *Journal of Polymer Research*, 2017, **24**, 1-10.
6. A. Aslan and A. Bozkurt, *Journal of Power Sources*, 2012, **217**, 158-163.
7. M. Farrokhi and M. Abdollahi, *European Polymer Journal*, 2020, **131**, 109691.
8. Y. Tokuda, S. Nishioka, Y. Ueda, H. Koyanaka, H. Masai, M. Takahashi and T. Yoko, *Solid State Ionics*, 2012, **225**, 232-235.